Quasilattice of fixed points of the fivefold stochastic web map

J. H. Lowenstein
Department of Physics, New York University, New York, New York 10003
(Received 27 May 1993)

The quasicrystalline properties of the fivefold stochastic web map M can be understood in terms of an extension of the map to five-dimensional space. The present work focuses on the construction of a lattice of special fixed points of the fifth-iterate map M^5 called quasicenters of tolerance ϵ. With the origin shifted to a quasicenter, M^5 resembles closely the unshifted map, with distortions of order ϵ everywhere in the phase space. The quasicenters are located by first constructing a quasilattice of reference points by the so-called direct-projection method. Exploiting periodicity in $\mathbb{R}^5$, the quasicenters themselves are determined, to arbitrary precision, by means of a convergent iterative scheme, and the diffraction pattern is found by evaluating a five-dimensional integral in the neighborhood of the origin. For representative parameter values, the convergence of the iterative process is established by computer-assisted interval analysis.

PACS number(s): 05.45.+b, 61.44.+p

I. INTRODUCTION

Numerical investigation [1–3] of the stochastic web map with approximate q-fold rotational symmetry reveal phase portraits with the apparent structure of a two-dimensional quasicrystal. For example, in the simplest case, a Penrose tiling [4] may be superimposed on the $q=5$ web map's phase portrait, with the arrangement of fixed points, invariant curves, stochastic layers, etc., forming an approximate decoration of the tiles [2]. In addition, the diffraction pattern associated, via Fourier transformation, with long chaotic orbits, is reminiscent of the pointlike diffraction pattern of the Ammann quasilattice [5–8] associated with the Penrose tiling.

A striking feature of the quasicrystalline structure generated by the web map is the existence of *quasicenters* [9]. These are special points in the plane that not only are stable fixed points of the qth iterate of the web map but also correspond to approximate invariance of the map with respect to certain translations. Thus, relative to a quasicenter, the qth iterate map acts in a way that closely resembles its action relative to the origin of coordinates. Figure 1 provides a good illustration. Here we have used a fifth-order interpolating Hamiltonian [10] to generate an accurate representation of the phase portrait of the fivefold web map over a fairly large area surrounding (a) the origin, and (b) a not too distant quasicenter. As we shall see later, it is possible to classify the quasicenters according to how well they mimic the origin. The collection of all quasicenters of a given "tolerance" will be seen to form an infinite two-dimensional quasicrystal.

The aim of the present work is to provide a detailed investigation of the quasicenters in the important case where $q=5$, relying on an important insight of Ref. [9]: the two-dimensional phase space of the web map can be embedded in a q-dimensional real space in such a way that periodicity in q dimensions is translated into quasiperiodicity in two dimensions.

The presentation is organized as follows. After a brief review, in Sec. II, of the basic features of the stochastic web map, we turn, in Sec. III, to a one-dimensional example that provides a convenient introduction to the methods relating to quasicrystals, which we apply later on. In Sec. IV, we discuss the embedding in five dimensions, reviewing the results of Ref. [9], and derive a precise statement of the approximate translational invariance. Before constructing the lattice of quasicenters, we build (in Sec. V) a simpler, more symmetric quasilattice by projecting onto the phase plane a set of sufficiently close *integer* lattice points in five dimensions. The formalism is a direct generalization of the one-dimensional model of Sec. III. The projected lattice points serve as a starting point for an iterative construction, presented in Sec. VI, of the quasicenters themselves. Formulas for the pointlike diffraction pattern associated with the lattice of quasicenters are derived in Sec. VII, and a computer-assisted proof, based on interval arithmetic, of the convergence of our iterative scheme is included in Sec. VIII (with the rules of interval analysis relegated to the Appendix). Section IX contains some concluding remarks.

II. PRELIMINARY CONSIDERATIONS

The fivefold web map, treated extensively by Zaslavsky and co-workers (for a detailed review, see [11] and [12]), is the Poincaré map of a harmonic oscillator kicked five times per natural period by a spatially sinusoidal impulsive force. Specifically, the points in phase space just prior to each kick are related by the map M defined by

$$M:\ \begin{pmatrix} x \\ y \end{pmatrix} \to \begin{pmatrix} \cos\alpha & \sin\alpha \\ -\sin\alpha & \cos\alpha \end{pmatrix} \begin{pmatrix} x \\ y + a\sin x \end{pmatrix}, \tag{1}$$

where a is proportional to the strength of the kick, and

$$\alpha = 2\pi/5 .$$

For $a \ll 1$, the dynamics of the fifth-iterate map M^5 is asymptotically close to a Hamiltonian flow

$$M^5 \begin{pmatrix} x \\ y \end{pmatrix} = \begin{pmatrix} x \\ y \end{pmatrix} + a \begin{pmatrix} \dfrac{\partial H}{\partial y} \\ -\dfrac{\partial H}{\partial x} \end{pmatrix} + O(a^2), \tag{2}$$

$$H(x,y)=\sum_{k=0}^{4}\cos(x\cos k\alpha+y\sin k\alpha)\ . \tag{3}$$

The main theme of our present investigation is the existence of certain invariant sets of the map M that have a quasicrystalline structure in the sense that we can associate with them phase-space density functions that are *quasiperiodic,* i.e., they have Fourier decompositions of the form

$$\rho(\mathbf{x})=\sum_{\mathbf{k}\in I}c_{\mathbf{k}}e^{i\mathbf{k}\cdot\mathbf{x}}\ , \tag{4}$$

where the set I of allowed wave vectors is generated by taking linear combinations, with integer coefficients, of a finite set of basis vectors. If the series (4) is uniformly convergent, ρ belongs to the space of almost periodic functions (see, for example, [13]). For our purposes, this class of functions is too restrictive, and so we prefer the more general framework of Refs. [14,15], considering ρ to be a class $\mathcal{S}'$ generalized function (tempered distribution). The latter is defined as a continuous linear functional on the space $\mathcal{S}$ of infinitely differentiable real-valued functions that decrease at infinity faster than any power of the distance from the origin. Thus $\rho\in\mathcal{S}'(\mathbb{R}^n)$ is *defined* by the integral

$$\rho(f)=\int d^n x\rho(x)f(x)\ .$$

We need not review the details of the topologies of $\mathcal{S}$ and $\mathcal{S}'$, but merely point out some useful results (see [15]). If $f\in\mathcal{S}$, then f has a Fourier transform that is also in $\mathcal{S}$. The analogous property holds for elements of $\mathcal{S}'$. Convergence to a series $\sum_i\rho_i$, $\rho_i\in\mathcal{S}'$, can be checked by showing that for arbitrary $f\in\mathcal{S}$, $\sum_i\rho_i$ converges as a series of real numbers. If $\rho=\sum_i\rho_i$ converges, then the expansion of the Fourier transform, $\tilde{\rho}=\sum_i\tilde{\rho}_i$, also converges.

A simple example to keep in mind as we proceed is the following (Ref. [15], p. 170). Clearly the Dirac delta function $\delta(x)$ is in $\mathcal{S}'$, with $\delta(f)=f(0)$. The series

$$\rho(x)=\sum_{n=0}^{\infty}\delta(x-2\pi n)$$

converges, since, if we take any $f\in\mathcal{S}$,

$$\rho(f)=\int f(x)\rho(x)dx$$

$$=\sum_{n=0}^{\infty}\int f(x)\delta(x-2\pi n)dx=\sum_{n=0}^{\infty}f(2\pi n)\ .$$

The last sum converges by virtue of the rapid decrease of f at ∞.

A convenient way [16,17] to construct a quasicrystal in d dimensions is to embed $\mathbb{R}^d$ in $\mathbb{R}^q$, $q>d$, in a special way. Let Z^q be the set of q vectors with integer components. Identify $\mathbb{R}^d$ with a d-dimensional subspace S oriented so that it intersects Z^q only in the origin. S is said to be *irrationally placed.* Now consider a generalized function $\rho(x)$ that is periodic in $\mathbb{R}^q$ (we arbitrarily select period 2π),

$$\rho(\zeta)=\rho(\zeta+2\pi\nu)\ ,\quad \nu\in Z^q\ ,$$

with a Fourier series expansion

$$\rho(\zeta)=\sum_{\kappa\in Z^q}c_\kappa e^{i\kappa\cdot\zeta}\ ,$$

where

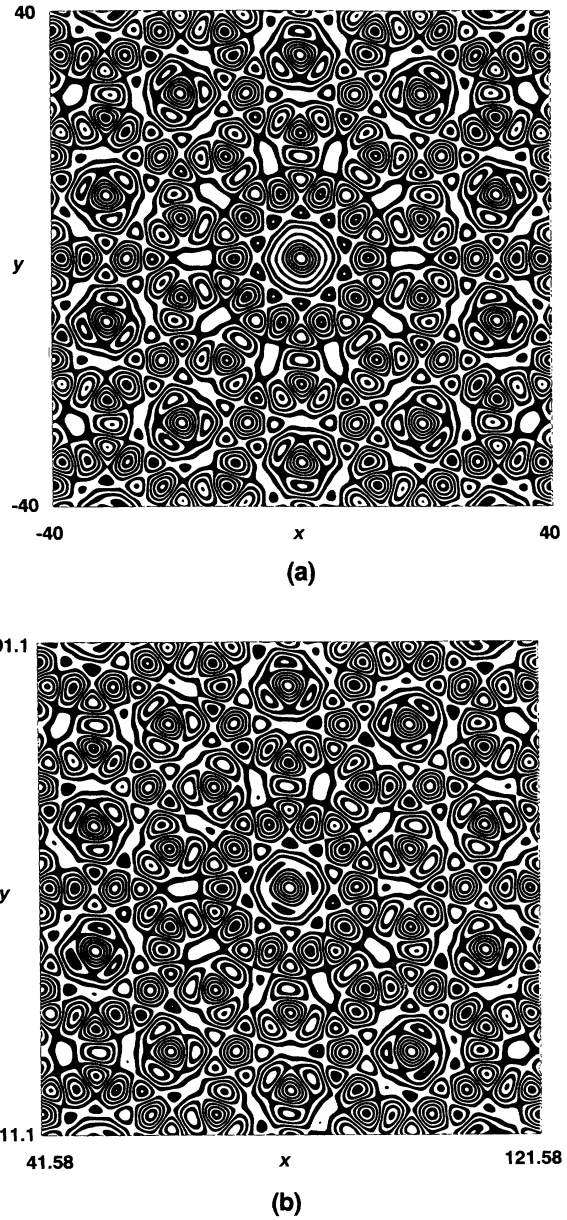

FIG. 1. Phase portraits of the $q=5$ web map ($a=0.3$) in two 80×80 regions of the xy plane, centered about the points (a) (0,0), and (b) (81.58,251.09). The latter lies very close to a quasicenter Q. In these figures, generated with the help of a fifth-order interpolating Hamiltonian [10], the black-white boundaries coincide, within the graphical resolution of these pictures, with closed invariant curves of the web map M. As we see in Sec. IV, one can find other quasicenters, much farther out in the plane, whose phase portraits are indistinguishable from (a) within the given resolution.

$$c_\kappa=(2\pi)^{-q}\int_{[-\pi,\pi]^q} d\zeta\,\rho(\zeta)e^{-i\kappa\cdot\zeta}\ .$$

Here we have chosen as fundamental domain the q-dimensional cube of side 2π centered at the origin. We assume that ρ can be restricted to S, in the sense that for $\zeta\in S$,

$$\rho_S(\zeta)\equiv\sum_{\kappa\in Z^q} c_\kappa e^{i\kappa\cdot\zeta}$$

converges as a generalized function in $\mathcal{S}'(S)$. Then we arrive at a quasiperiodic generalized function of the form (4) by making a transformation to new variables intrinsic to S:

$$\zeta=\xi(\mathbf{x}),\quad \mathbf{x}\in\mathbb{R}^d\ ,$$

$$r(\mathbf{x})=\rho_S(\xi(\mathbf{x}))=\sum_{\mathbf{k}} C_{\mathbf{k}}e^{i\mathbf{k}\cdot\mathbf{x}}\ ,$$

where

$$C_{\mathbf{k}}=\sum_{\xi(\mathbf{k})=\phi_S(\kappa)} c_\kappa\ .$$

Since the restriction of a class $\mathcal{S}'$ generalized function to a subspace is not automatically well defined, one must check explicitly that the indicated expansion of $r(\mathbf{x})$ is meaningful.

We conclude this brief presentation of mathematical tools with mention of some properties of the golden mean,

$$\tau=\frac{1+\sqrt{5}}{2}\ , \tag{5}$$

and the related sequence of integers, the Fibonacci sequence defined by

$$F_0=F_1=1,\ldots,F_{n+1}=F_n+F_{n-1},\ldots\ . \tag{6}$$

The properties that we use in the present work are straightforward applications of these definitions and the identities

$$\tau^2=\tau+1\ , \tag{7}$$

$$F_k=\frac{1}{3-\tau}(\tau^k+(-1)^k\tau^{-k-2})\ , \tag{8}$$

$$\tau F_k-F_{k+1}=(-1)^k\tau^{-k-1}\ . \tag{9}$$

It is also convenient to recall that any positive integer n can be expanded as a sum of distinct Fibonacci numbers,

$$n=\sum_{k=1} c_k F_k\ , \tag{10}$$

with

$$c_k\in\{0,1\},\quad c_{k+1}c_k=0\ .$$

Because it appears frequently in expressions for bounds and vector norms, we shall consistently use the notation

$$\sigma\equiv 3-\tau=1+\tau^{-2}\ . \tag{11}$$

III. CONSTRUCTION OF A ONE-DIMENSIONAL QUASICRYSTAL

In this section we present a simple example of the method of constructing a quasiperiodic (generalized) function described in the previous section. The example is chosen to introduce much of the machinery that we use later as well as to make a connection with a well-known method from the theory of quasicrystals, the so-called *direct-projection method* [16–20].

We begin by defining a generalized function f_0 with support in the unit square:

$$f_0(\zeta)=\sigma\delta(\zeta_1+\zeta_2/\tau)\theta(\zeta_2-\zeta_1/\tau+b)\times\theta(b-\zeta_2+\zeta_1/\tau)\ ,$$

$$-\tfrac{1}{2}<\zeta_1,\ \zeta_2<\tfrac{1}{2},\quad 0<b<\frac{\sigma}{2}\ . \tag{12}$$

The support of f_0 (see Fig. 2) has been chosen to lie in the subspace $S_\perp$ perpendicular to the subspace

$$S=\{(x,x/\tau):-\infty<x<\infty\}\ , \tag{13}$$

where τ is the golden mean. This is easily extended to a periodic function (see Fig. 3) on $\mathbb{R}^2$,

$$f(\zeta)=\sum_{\nu\in Z^2} f_0(\zeta-\nu)\ , \tag{14}$$

which satisfies

$$f(\zeta+\nu)=f(\zeta)\ ,\quad \nu\in Z^2\ . \tag{15}$$

It is convenient to introduce coordinates x and u intrinsic to S and $S_\perp$, respectively. Thus, we make the linear transformation

$$\zeta(x,u)=(x-u/\tau,\ x/\tau+u) \tag{16}$$

and reexpress f_0 and f in terms of the new coordinates:

$$\varphi_0(x,u)\equiv f_0(\zeta(x,u))=\delta(x)\theta(u+u_1)\theta(u_1-u)\ , \tag{17}$$

where $u_1=b/\sigma$, and

$$\varphi(x,u)\equiv f(\zeta(x,u))\ . \tag{18}$$

The restriction of $f(\zeta)$ to S gives a quasiperiodic sum of δ

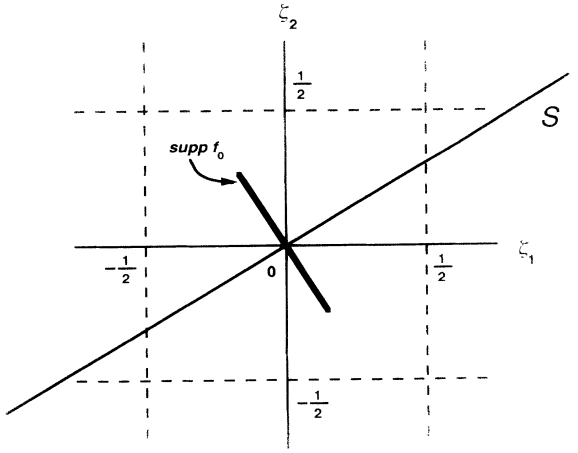

FIG. 2. Support of f_0.

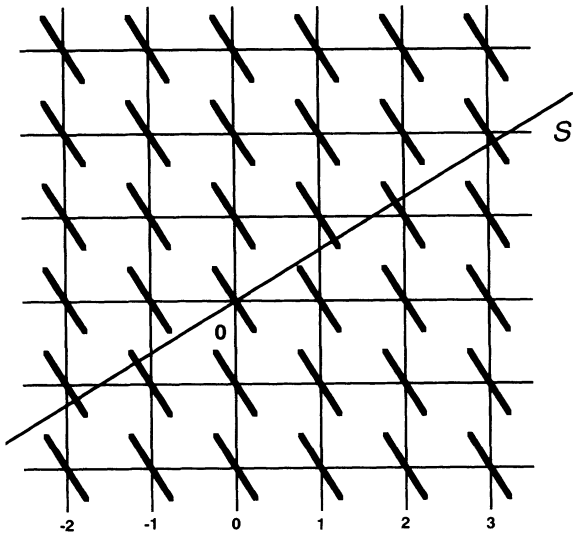

FIG. 3. Support of f. The restriction of f to S, namely $\rho(x)$, is supported on $\mathrm{supp}f \cap S$.

functions,

$$\rho(x)\equiv\varphi(x,0)=\delta(x)+\sum_{n=1}(\delta(x-x_n)+\delta(x+x_n)) , \tag{19}$$

which may be regarded as the density of an ideal quasicrystal with a pointlike "atom" at each of the intersections $0,\pm x_n$, $n=1,2,\ldots$ of S with the support of f. Another way of identifying these points is as the orthogonal projections onto S of all integer lattice points within a strip of width $2b/\sqrt{\sigma}$ centered about S. Our construction thus differs little from the direct-projection method [16–20], which was studied extensively in the mid 1980s. In our case the assumptions of inversion symmetry and choice of τ^{-1} for the irrational slope of S have been motivated by our eventual application to the fivefold web map.

To display explicitly the quasiperiodicity of $\rho(x)$, we must show that it can be expanded as a suitable discrete sum of exponentials $\exp ikx$. According to our general strategy, we simply restrict to S the Fourier series representing $f(\xi)$:

$$f(\xi)=\sum_{m,n} c_{mn} e^{2\pi i(m\xi_1+n\xi_2)} , \tag{20}$$

where

$$c_{mn}=\int_{-1/2}^{1/2} d\xi_1 \int_{-1/2}^{1/2} d\xi_2 f(\xi_1,\xi_2) e^{-2\pi i(m\xi_1+n\xi_2)} \tag{21}$$

$$=\frac{\sigma}{\pi(n-m/\tau)}\sin[2\pi(n-m_0/\tau)u_1] , \tag{22}$$

so that

$$\rho(x)=f(\xi(x,0))=\sum_{m,n} c_{mn} e^{-2\pi i k_{m,n} x} , \tag{23}$$

with

$$k_{mn}=m+n/\tau . \tag{24}$$

To obtain an explicit expression for the location of the δ functions comprised by $\rho(x)$, we note that the line S intersects each line $\xi_1=m$, $m\in Z$, in a point m/τ lying between consecutive integer values $\lfloor m/\tau \rfloor$ (floor) and $\lceil m/\tau \rceil$ (ceiling), as depicted in Fig. 4. Every point in the support of ρ is the projection on S on one of the bracketing integer lattice points, either $(m,\lfloor m/\tau \rfloor)$ or $(m,\lceil m/\tau \rceil)$. The projections are, respectively,

$$q_-(m)=\frac{1}{\sigma}\left[m+\frac{1}{\tau}\left\lfloor\frac{m}{\tau}\right\rfloor\right] \tag{25}$$

and

$$q_+(m)=\frac{1}{\sigma}\left[m+\frac{1}{\tau}\left\lceil\frac{m}{\tau}\right\rceil\right] , \tag{26}$$

with geometrical bounds given by

$$q_\pm(m)=m+\langle\langle q_\pm(m)\rangle\rangle , \tag{27}$$

$$-\frac{1}{\tau\sigma}<\langle\langle q_-(m)\rangle\rangle<0<\langle\langle q_+(m)\rangle\rangle<\frac{1}{\tau\sigma} , \tag{28}$$

and the inversion property

$$q_\pm(-m)=-q_\mp(m) . \tag{29}$$

Here we have used the notation $\langle\langle r\rangle\rangle$ to denote the difference between the real number r and the nearest integer, i.e.,

$$\langle\langle r\rangle\rangle\equiv\lfloor r+\tfrac{1}{2}\rfloor . \tag{30}$$

Since

$$q_+(m)-q_-(m)=\frac{1}{\tau\sigma} ,$$

at most one member of the pair $(q_\pm,q_\pm/\tau)$ is sufficiently close to an integer lattice point to intersect $\mathrm{supp}f$. For sufficiently small $\langle\langle q_\pm(m)\rangle\rangle$, namely,

$$|\langle\langle q_\pm(m)\rangle\rangle|<\frac{1}{\tau^3\sigma} ,$$

the quantity

$$q(m)=m+\langle\langle q(m)\rangle\rangle , \tag{31}$$

with

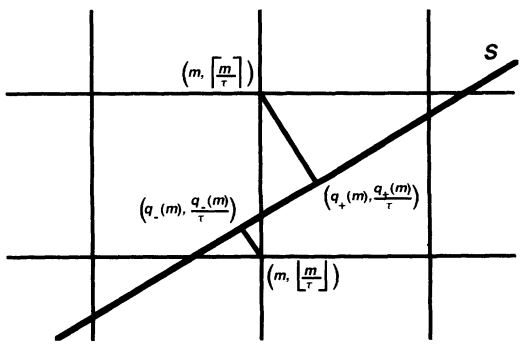

FIG. 4. Bracketing of the point $(m,m/\tau)$ by $(m,\lfloor m/\tau \rfloor)$ and $(m,\lceil m/\tau \rceil)$.

$$\langle\langle q(m)\rangle\rangle = -\left\langle\left\langle \frac{m}{\tau}\right\rangle\right\rangle \Big/ \sqrt{5} \ , \tag{32}$$

coincides with the relevant $q_+(m)$ or $q_-(m)$:

$$q(m) = \begin{cases} q_-(m), & -\tau^{-3}\sigma^{-1} < \langle\langle q_-(m)\rangle\rangle \le 0 \\ q_+(m), & 0 \le \langle\langle q_-(m)\rangle\rangle < \tau^{-3}\sigma^{-1} \ . \end{cases} \tag{33}$$

Now $q(m)$ has some useful properties that favor its usage for $|u_1| < \tau^{-3}\sigma^{-1}$ in (17) [i.e., $b < \tau^{-3}$ in (12)]. In particular, if we make a Fibonacci expansion of the integer m,

$$m = \sum_{k=1} c_k F_k, \quad c_k \in \{0,1\}, \quad c_k c_{k+1} = 0 \ ,$$

then

$$q(m) = \frac{1}{\sigma}\left[m + \frac{1}{\tau}\left\lfloor \frac{m+1}{\tau} \right\rfloor \right] = \frac{1}{\sigma}\sum_{k=1} c_k \tau^k \ , \tag{34}$$

$$\langle\langle q(m)\rangle\rangle = q(m) - m = \frac{1}{\sigma}\sum_{k=1} c_k (-1)^{k+1}\tau^{-k-2} \ . \tag{35}$$

From (35), we verify that if $c_i = 0$, $i = 1, \ldots, L-1$, $c_L = 1$, then

$$\frac{1}{\tau^{L+3}\sigma} < |\langle\langle q(m)\rangle\rangle| < \frac{1}{\tau^{L+1}\sigma} \ . \tag{36}$$

In order that $x = q(m)$ be in the support of $\rho(x)$, we must have

$$|\langle\langle q(m)\rangle\rangle| = \frac{|u|}{\tau} < \frac{u_1}{\tau} \ , \tag{37}$$

that is, m must satisfy the condition

$$\left| \left\langle\left\langle \frac{m}{\tau}\right\rangle\right\rangle \right| < u_1\sigma = b \ . \tag{38}$$

From the inequalities (36), we see that if

$$m = \sum_{k=L} c_k F_k \ , \tag{39}$$

a necessary condition for $q(m) \in \text{supp}\rho$ is

$$\tau^{-L-2} < b \ , \tag{40}$$

while a sufficient condition is

$$\tau^{-L} < b \ . \tag{41}$$

We close this section with a useful scaling property of the numbers $q(m)$: multiplication by τ brings one closer to an integer by a factor $-\tau^{-1}$:

$$\langle\langle q(n)\tau\rangle\rangle = -\tau^{-1}\langle\langle q(n)\rangle\rangle \ . \tag{42}$$

By similar reasoning,

$$\langle\langle q(n)/\tau\rangle\rangle = -\tau\langle\langle q(n)\rangle\rangle \ . \tag{43}$$

IV. FIVE-DIMENSIONAL EMBEDDING

Extending the $q = 5$ web map [9] in a useful way to a periodic map in five-dimensional space ($\mathbb{R}^5$) depends crucially on the properties of the cyclic permutation P_5, defined by

$$P_5 : (\zeta_0, \ldots, \zeta_4) \to (\zeta_1, \ldots, \zeta_4, \zeta_0) \ , \tag{44}$$

or, in matrix notation,

$$P_5 = \begin{vmatrix} 0 & 1 & 0 & 0 & 0 \\ 0 & 0 & 1 & 0 & 0 \\ 0 & 0 & 0 & 1 & 0 \\ 0 & 0 & 0 & 0 & 1 \\ 1 & 0 & 0 & 0 & 0 \end{vmatrix} \ .$$

Within $\mathbb{R}^5$, this linear transformation has three mutually orthogonal invariant subspaces:

$$X = \{\xi(x,y) : -\infty < x,y < \infty\} \ , \tag{45}$$

$$U = \{\eta(u,v) : -\infty < u,v < \infty\} \ , \tag{46}$$

$$W = \{\psi(w) : -\infty < w < \infty\} \ , \tag{47}$$

where

$$\xi(x,y) = x\omega^{(1)} + y\omega^{(2)} \ , \tag{48}$$

$$\eta(u,v) = u\omega^{(3)} + v\omega^{(4)} \ , \tag{49}$$

$$\psi(w) = w\omega^{(5)} \ , \tag{50}$$

and the (unnormalized) basis vectors $\omega^{(k)}$ are

$$\omega^{(1)} = (1, \cos\alpha, \cos 2\alpha, \cos 2\alpha, \cos\alpha) \ , \tag{51}$$

$$\omega^{(2)} = (0, \sin\alpha, \sin 2\alpha, -\sin 2\alpha, -\sin\alpha) \ , \tag{52}$$

$$\omega^{(3)} = (1, \cos 2\alpha, \cos\alpha, \cos\alpha, \cos 2\alpha) \ , \tag{53}$$

$$\omega^{(4)} = (0, \sin 2\alpha, -\sin\alpha, \sin\alpha, -\sin 2\alpha) \ , \tag{54}$$

$$\omega^{(5)} = (1,1,1,1,1) \ . \tag{55}$$

Essential to the construction is the fact that X, which is to be identified with the two-dimensional phase space of the web map, is irrationally placed, i.e., the only real x and y for which all five components of

$$\xi(x,y) = \begin{vmatrix} x \\ x\cos\alpha + y\sin\alpha \\ x\cos 2\alpha + y\sin 2\alpha \\ x\cos 2\alpha - y\sin 2\alpha \\ x\cos\alpha - y\sin\alpha \end{vmatrix} \tag{56}$$

are integer multiples of 2π are $x = 0$ and $y = 0$. The same property obviously holds for the orthogonal subspace U, but not for W (which contains all points of the form

$$2\pi m\omega^{(5)} \equiv (2\pi m, 2\pi m, \ldots, 2\pi m), \quad m \in Z \ .$$

In what follows, we consistently use $\mathbf{x} \equiv (x,y)$ and $\mathbf{u} \equiv (u,v)$ to parametrize X and U, respectively, and write $\xi(\mathbf{x})$ and $\eta(\mathbf{u})$ for the $\mathbb{R}^2 \to \mathbb{R}^5$ embedding transformations (48)–(50). Within the respective invariant subspaces, X, U, and W, P_5 acts as follows:

$$\mathbf{x} \to R(\alpha)\mathbf{x} \ , \tag{57}$$

$$\mathbf{u} \to R(2\alpha)\mathbf{u} \ , \tag{58}$$

$$w \to w \ , \tag{59}$$

where $R(\theta)$ is the two-dimensional clockwise rotation by angle θ.

It is now easy to write the five-dimensional analog of M:

$$M_5(\zeta)=P_5(\zeta+a\sin\zeta_0\omega^{(2)}) . \tag{60}$$

We see immediately that M_5 leaves the subspace X invariant, and within X it acts as M:

$$M_5(\xi(\mathbf{x}))=\xi(M(\mathbf{x})) . \tag{61}$$

(Recall that ξ simply shifts from the rectangular coordinates x, y intrinsic to X to the corresponding five-vector coordinates in the embedding space.) The translation invariance property of M_5, or more accurately its fifth-iterate map M_5^5, follows [9] directly from (60): for all integer lattice points $\nu=(\nu_0,\ldots,\nu_4)\in Z^5$, and arbitrary point $\zeta\in\mathbb{R}^5$,

$$M_5(\zeta+2\pi\nu)=M_5(\zeta)+2\pi P_5\nu , \tag{62}$$

and hence

$$M_5^5(\zeta+2\pi\nu)=M_5^5(\zeta) . \tag{63}$$

Another useful translational property of M_5 is the following: for all $\xi(\mathbf{x}),\xi(\mathbf{x}')\in X$, and $\chi\in X_\perp\equiv U\otimes W$,

$$M_5(\xi(\mathbf{x})+\xi(\mathbf{x}')+\chi)=\xi(\tilde{M}_{\xi(\mathbf{x}')_0+\chi_0}(\mathbf{x}))+P_5\chi , \tag{64}$$

with

$$\tilde{M}_z(\mathbf{x})\equiv R(\alpha)\begin{pmatrix} x \\ y+a\sin(z+x)\end{pmatrix} . \tag{65}$$

Hence

$$M_5^5(\xi(\mathbf{x})+\xi(\mathbf{x}')+\chi)=\xi(\tilde{M}^{(5)}_{\xi(\mathbf{x}')+\chi}(\mathbf{x}))+\chi , \tag{66}$$

where

$$\tilde{M}^{(5)}_\zeta=\tilde{M}_{\zeta_4}\circ\cdots\circ\tilde{M}_{\zeta_0} . \tag{67}$$

From (66), we see that M_5^5 leaves invariant not only X, but also every hyperplane

$$\chi+X\equiv\{\chi+\zeta:\zeta\in X\}=\{\chi+\xi(\mathbf{x}):\mathbf{x}\in\mathbb{R}^2\}$$

parallel to X. Within $\chi+X$, M_5^5 acts simply as $\tilde{M}^{(5)}_\chi$.

But (66) also describes translations within X, i.e., $\mathbf{x}\to\mathbf{x}+\mathbf{x}'$. We see that $\tilde{M}^{(5)}_{\xi(\mathbf{x}')}$ plays the role of the fifth-iterate map *relative to the shifted origin* $\mathbf{x}'$. One of the expressions of the quasiperiodicity of M^5 is a restricted form of translation invariance; there exist special shifts $\mathbf{x}'$ such that the relative map $\tilde{M}^{(5)}_{\xi(\mathbf{x}')}$ and the original one, M^5, are almost indistinguishable. This can be seen from the explicit forms of $\tilde{M}_{\zeta_0}$ in (65) and $\tilde{M}^5_\zeta$ in (67): if all five of the ζ_k are close to integer multiples of 2π, i.e., $\zeta\approx2\pi\nu$, $\nu\in Z^5$, then each factor in the definition of $\tilde{M}^{(5)}_\zeta$ acts very much like M, and so $\tilde{M}^{(5)}_\zeta$ acts very much like M^5.

A precise statement of the closeness of $\tilde{M}^{(5)}_\zeta$ and M^5 is the following: for all $\mathbf{x}\in\mathbb{R}^2,\zeta\in\mathbb{R}^5$,

$$|\tilde{M}^{(5)}_\zeta\mathbf{x}-M^5\mathbf{x}|<a\sum_{k=0}^{4}(1+a)^{4-k}|\langle\zeta_k\rangle| , \tag{68}$$

where, for any real r,

$$\langle r\rangle\equiv2\pi\langle\langle r/(2\pi)\rangle\rangle . \tag{69}$$

Here the double bracket is the signed fractional part introduced in (30).

Proof of estimate (68). The proof is based on the mean-value theorem of differential calculus:

$$\begin{aligned}\delta\mathbf{x}'&\equiv\tilde{M}_z(\mathbf{x}+\delta\mathbf{x})-M(\mathbf{x})\\&=R(\alpha)\delta\mathbf{x}+aR(\alpha)\begin{pmatrix}0\\ \sin(\langle z\rangle+\delta x+x)-\sin x\end{pmatrix}\\&=R(\alpha)\delta\mathbf{x}+a(\langle z\rangle+\delta x)\cos(x+\Delta x)\begin{pmatrix}\sin\alpha\\ \cos\alpha\end{pmatrix} ,\end{aligned} \tag{70}$$

with

$$0\le\Delta x\le\langle z\rangle+\delta x ,$$

which implies, by the triangle inequality,

$$|\delta\mathbf{x}'|\le(1+a)|\delta\mathbf{x}|+a|\langle z\rangle| . \tag{71}$$

Applying $\tilde{M}_{\zeta_0},\ldots,\tilde{M}_{\zeta_4}$, in that order, on $\mathbf{x}$, we have from (71)

$$|\tilde{M}_{\zeta_0}\mathbf{x}-M\mathbf{x}|\le a|\langle\zeta_0\rangle| ,$$

$$|\tilde{M}_{\zeta_1}\circ\tilde{M}_{\zeta_0}(\mathbf{x})-M^2(\mathbf{x})|\le a(1+a)|\langle\zeta_0\rangle|+a|\langle\zeta_1\rangle| ,$$

and finally,

$$\begin{aligned}&|\tilde{M}_{\zeta_4}\circ\cdots\circ\tilde{M}_{\zeta_0}(\mathbf{x})-M^5(\mathbf{x})|\\&\qquad\le a((1+a)^4|\langle\zeta_0\rangle|+\cdots+|\langle\zeta_4\rangle|).\end{aligned}$$ □

V. PROJECTED FIVE-DIMENSIONAL LATTICE POINTS

We saw in the previous section that points of phase space, which, when embedded in five-dimensional space as in (45), lie close to a lattice point $(2\pi\nu_0,\ldots,2\pi\nu_4)$, ν_k integer, are special; the phase portrait of M^5 relative to them resembles that relative to the origin (0,0). In the remainder of this work we focus on such points. First, we locate explicitly the points of closest approach, i.e., the orthogonal projections of nearby lattice points onto X. Unlike the origin, these are not fixed points of the map, but it turns out that they are very close to such fixed points. We find that both the set of projected lattice points and the nearby fixed points of M^5 (*quasicenters*) are, in the formal sense, two-dimensional quasicrystals closely related to the one-dimensional example of Sec. III. In fact, much of the formalism developed there is directly applicable.

Using the basis vectors $\omega^{(k)}$ in (51)–(55), the invariant decomposition of $\mathbb{R}^5$ takes the form

$$\zeta=\phi_X(\zeta)+\phi_U(\zeta)+\phi_W(\zeta) , \tag{72}$$

where

$$\phi_X(\zeta)=\tfrac{2}{5}[(\zeta\cdot\omega^{(1)})\omega^{(1)}+(\zeta\cdot\omega^{(2)})\omega^{(2)}] , \tag{73}$$

$$\phi_U(\zeta)=\tfrac{2}{5}[(\zeta\cdot\omega^{(3)})\omega^{(3)}+(\zeta\cdot\omega^{(4)})\omega^{(4)}] , \tag{74}$$

$$\phi_W(\zeta)=\tfrac{1}{5}(\zeta\cdot\omega^{(5)})\omega^{(5)} . \tag{75}$$

If $\zeta \in X$, then $\phi_U(\zeta)=0$ and $\phi_W(\zeta)=0$. This places three linear constraints on the five ζ_i, leaving two independent coordinates, say ζ_0 and ζ_2, with the remaining ones determined by

$$\zeta_1=\tau(\zeta_0+\zeta_2) , \tag{76}$$

$$\zeta_3=-\tau\zeta_0-\zeta_2 , \tag{77}$$

$$\zeta_4=-\zeta_0-\tau\zeta_2 . \tag{78}$$

Now a lattice point $2\pi\nu$ very close to X will have components that *almost* satisfy (76)–(78). In particular, both $\tau\nu_0$ and $\tau\nu_2$ will be close to integers, the discrepancies being written (notation of Sec. III) $\langle\langle \tau\nu_k \rangle\rangle = \langle\langle \nu_k/\tau \rangle\rangle$, $k=0, 2$. Moreover,

$$\nu_1=\tau(\nu_0+\nu_2)-\langle\langle \nu_0/\tau \rangle\rangle - \langle\langle \nu_2/\tau \rangle\rangle , \tag{79}$$

$$\nu_3=-\tau\nu_0-\nu_2+\langle\langle \nu_0/\tau \rangle\rangle , \tag{80}$$

$$\nu_4=-\nu_0-\tau\nu_2+\langle\langle \nu_2/\tau \rangle\rangle . \tag{81}$$

Substituting (79)–(81) into (73) and rearranging terms, we get for the projected lattice point

$$2\pi\phi_X(\nu)=2\pi(q(\nu_0), \ldots, q(\nu_4)) , \tag{82}$$

with

$$q(m)=m+\langle\langle q(m) \rangle\rangle ,$$

and

$$\langle\langle q(m) \rangle\rangle = -\langle\langle m/\tau \rangle\rangle /\sqrt{5} .$$

The orthogonal displacement of the subspace X from $2\pi\nu$ is

$$\chi=-2\pi\phi_U(\nu)=2\pi(\langle\langle q(\nu_0) \rangle\rangle, \ldots, \langle\langle q(\nu_4) \rangle\rangle) , \tag{83}$$

with components linked by [the analog in U of (76)–(78)]

$$\chi_1=-\tau^{-1}(\chi_0+\chi_2) , \tag{84}$$

$$\chi_3=\tau^{-1}\chi_0-\chi_2 , \tag{85}$$

$$\chi_4=-\chi_0+\tau^{-1}\chi_2 . \tag{86}$$

Note that the restriction that the lattice point $2\pi\nu$ be close to X automatically ensures that $\phi_W(\nu)=0$, and so χ can be parametrized by the two rectangular coordinates in U, namely u and v.

Consider now the set Π_ϵ of all points of X of the form (82) such that the distance to the nearest lattice point $2\pi\nu$ (namely, $|\eta(\nu)|$) is less than or equal to ϵ. To see that Π_ϵ is a quasiperiodic array, we can apply the same reasoning as in Sec. III. The set

$$\{\chi+2\pi\nu : \nu\in Z^5, \chi\in X_\perp, |\chi|\le\epsilon\}$$

is obviously periodic with period 2π in each coordinate direction. Moreover, Π_ϵ is just the intersection of this set with X. This is sufficient to establish the quasiperiodicity.

Another way of thinking about the set Π_ϵ is in terms of a pentagrid construction in the xy plane. Let us draw the five one-dimensional grids,

$$\mathbf{e}_i\cdot\mathbf{x}=2\pi q(n), \quad i=0, \ldots, 4 , \tag{87}$$

where

$$\mathbf{e}_k=(\cos k\alpha, \sin k\alpha) ,$$

and n ranges over all integers such that

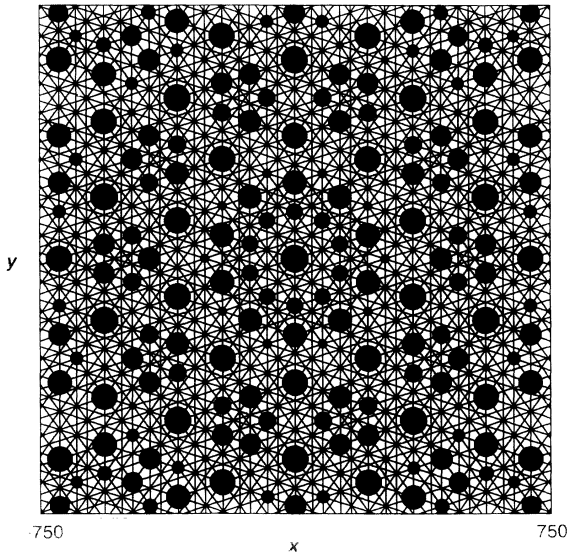

(a)

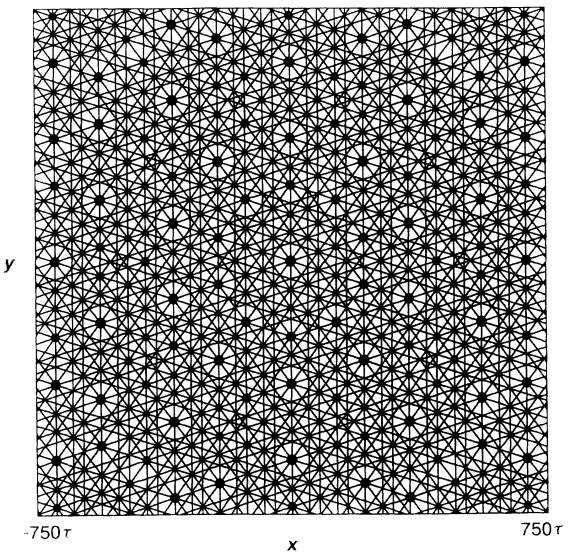

(b)

FIG. 5. Quasilattice Π_ϵ of projected integer lattice points of tolerance (a) $\epsilon=1/5$ and (b) $\epsilon=1/(5\tau)$. These are seen to lie at the mutual intersection points of five symmetrically placed one-dimensional grids. The collection of disks shown in the picture represent the intersections of the two-dimensional subspace X with the five-dimensional geometrical object obtained by placing a 5D ball of radius ϵ at every integer lattice site. The projections of the integer lattice sites are thus the centers of the disks. The disks have been enlarged by a factor of 200 to aid the eye. The lines, on the other hand, are the intersections of X with hyperplanes $\zeta_k=$const, spaced as in the one-dimensional quasicrystal of Sec. III, with $b/\sqrt{\sigma}=\epsilon$. The scales of the two pictures differ by a factor τ in order to make obvious the scale invariance of Π_ϵ and the associated pentagrid.

$$\left|\left\langle\!\left\langle \frac{n}{\tau} \right\rangle\!\right\rangle\right| \leq \frac{\epsilon\sqrt{5}}{2\pi} . \tag{88}$$

Then Π_ϵ is a subset of the mutual intersection points of all five grids [it is a proper subset, since the distance constraint defining Π_ϵ is stronger than the componentwise constraint (88)].

The quasicrystalline structure of Π_ϵ is illustrated in Fig. 5. In that picture, the projected lattice points of tolerance ϵ are located at the centers of the various disks, with the five families of associated grid lines shown in the background. The disks are generated by imagining each five-dimensional lattice point $2\pi\nu$ surrounded by a sphere of radius ϵ; the disks are the intersections of the spheres with X. If in a certain neighborhood the orthogonal displacement of X from $2\pi\nu$ is χ, with $|\chi| \leq \epsilon$, then the corresponding disk is of radius $\sqrt{\epsilon^2-|\chi|^2}$. For display purposes, we enlarge each disk by a factor of 200.

The set Π_ϵ and the associated pentagrid possess certain important symmetries: invariance with respect to $2\pi/5$ rotations, reflections with respect to any of the directions $\mathbf{e}_k$, and rescaling by a factor τ:

$$\Pi_{\epsilon/\tau} = \tau\Pi_\epsilon , \tag{89}$$

with an analogous property of the associated pentagrid. The scaling ("deflation" [7]) property of both sets is immediately evident in a comparison of frames (a) and (b) of Fig. 5.

The phase portrait in the neighborhood of a sample projected lattice point [near $\nu = 2\pi(13,42,13,-34,-34)$] is shown in Fig. 6. We note the presence of a stable fixed point of M^5 slightly displaced from the projected lattice point in the center. The set of such fixed points (quasicenters) is the subject of the next section. We see that in passing from the projected lattice points to the quasicenters, we must give up most of the symmetries just mentioned, but in spite of this, the quasicrystalline character of the array remains.

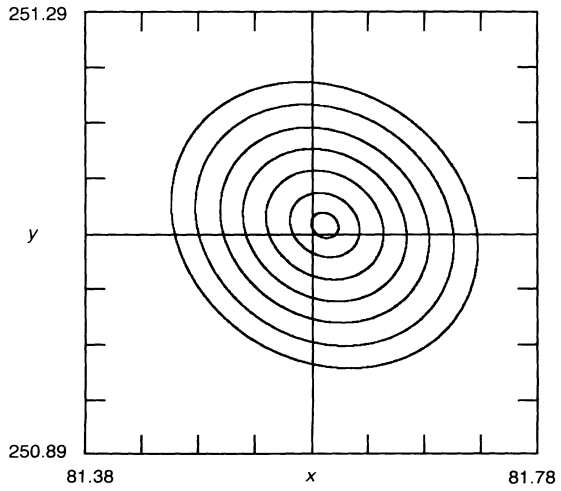

FIG. 6. Phase portrait of the web map ($a = 0.3$) in the neighborhood of the projected lattice point near $2\pi\nu$, $\nu = (13,42,13,-34,-34)$. The stable fixed point is the associated quasicenter.

VI. QUASICENTERS OF TOLERANCE ϵ

In the last section we constructed a quasilattice of phase-space points that lie within a distance ϵ of five-dimensional integer lattice points $2\pi\nu$, $\nu \in Z^5$. As we shall soon see, the situation shown in Fig. 6 is typical: near each of these projected lattice points there is a fixed point of M^5, which we have named a *quasicenter of tolerance* ϵ. Moreover, it will be shown that these shifted origins of the phase portrait form a quasiperiodic array in their own right. The geometrical relation of lattice point, projected lattice point, and quasicenter is indicated schematically in Fig. 7. This diagram shows the vicinity of a lattice point $2\pi\nu$, which is separated from the irrationally placed phase space X by a displacement $\chi \in U$. The coordinates of χ are $2\pi\langle\!\langle q(\nu_k)\rangle\!\rangle$, and those of the projected lattice point $\chi + 2\pi\nu$ are $2\pi q(\nu_k)$. It is easy to imagine this scenario translated to the vicinity of the origin, where the position of the fixed point $\mathbf{x}^*$ is a solution of the equation

$$\tilde{M}^{(5)}_{\eta(\mathbf{u})+\xi(\mathbf{x}^*)}(\mathbf{0}) = \tilde{M}^{(5)}_{\eta(\mathbf{u})}(\mathbf{x}^*) - \mathbf{x}^* = \mathbf{0} . \tag{90}$$

For $\mathbf{u} = \mathbf{0}$, this equation has the trivial solution

$$\mathbf{x}^*(\mathbf{0}) = \mathbf{0} ,$$

and, moreover, its Jacobian determinant there is nonvanishing:

$$\det[1 - DM^5(\mathbf{0})] \neq 0, \quad 0 < a < 1 .$$

By the implicit function theorem, there is a unique solution $\mathbf{x}^*(u,v)$ of (90) in some neighborhood

$$|\eta(u,v)| \equiv \sqrt{\tfrac{5}{2}}|\mathbf{u}| < \delta .$$

The solution set defines a smooth two-dimensional manifold

$$\mathcal{F}_\delta(0) = \{\eta(\mathbf{u}) + \xi(\mathbf{x}^*) : |\eta(\mathbf{u})| < \delta\} .$$

By translation invariance, for $\nu \in Z^5$,

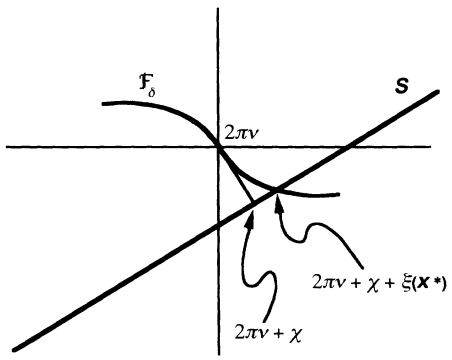

FIG. 7. Sketch of the vicinity of an integer lattice point $2\pi\nu$ located close to the irrationally placed subspace X (identified with phase space). In reality, the embedding space is five dimensional, and X is two dimensional, intersecting the two-dimensional fixed-point manifold $\mathcal{F}_\delta$ in a single point, the quasicenter. By means of a translation by $-2\pi\nu$, one can shift the entire configuration to a neighborhood of the origin.

$$\mathcal{J}_\delta(2\pi\nu)\equiv 2\pi\nu+\mathcal{J}_\delta(0)$$

is also a manifold of fixed points of M_5^5, depicted schematically by the curve in Fig. 7. Its intersection with X is then the quasicenter of tolerance ϵ associated with ν. Taking the union over all ν defines a periodic set of fixed points of M_5^5 whose restriction to X is the quasiperiodic array of quasicenters of tolerance ϵ.

A systematic recursion scheme for determining $\mathbf{x}^*(u,v)$ is the following:

$$\mathbf{x}^{*(0)}=\mathbf{0}\ , \tag{91}$$

$$\mathbf{x}^{*(n+1)}=\mathbf{x}^{*(n)}+\delta\mathbf{x}^{(n)}\ , \tag{92}$$

$$\delta\mathbf{x}^{(n)}\equiv G_0\tilde{M}^{(5)}_{\eta(\mathbf{u})+\xi(\mathbf{x}^{*(n)})}(\mathbf{0})\ , \tag{93}$$

$$G_\zeta\equiv-(D\tilde{M}^{(5)}_\zeta(\mathbf{0}))^{-1}\ . \tag{94}$$

This is closely related to Newton's root-finding method in $\mathbb{R}^2$ (for which G_0 would be replaced by $G_{\eta(\mathbf{u})+\xi(\mathbf{x}^{*(n)})}$). The use of a constant matrix G_0 makes (92) particularly appropriate for the systematic extraction of Taylor coefficients of $\mathbf{x}^*(u,v)$, as well as for the rigorous proof of convergence which we discuss in Sec. VIII below. We note that the first-order approximation

$$\mathbf{x}^{*(1)}=\delta\mathbf{x}^{(0)}=G_0\tilde{M}^{(5)}_{\eta(\mathbf{u})}(\mathbf{0})$$

gives an expression that correctly reproduces the linear approximation to the fixed-point manifold, with an error of order $|\eta(\mathbf{u})|^3$ (by inversion symmetry, only odd powers of u and v are encountered). Specifically,

$$x^{*(1)}(u,v)=\sum_{m+n\,\mathrm{odd}}A_{mn}u^mv^n=A_{10}u+A_{01}v+O(|\mathbf{u}|^3)\ , \tag{95}$$

$$y^{*(1)}(u,v)=\sum_{m+n\,\mathrm{odd}}B_{mn}u^mv^n=B_{10}u+B_{01}v+O(|\mathbf{u}|^3)\ , \tag{96}$$

where

$$A_{10}=4s(5-8s^2)a-(5-8s^2)a^2-s(1-4s^2)a^3\ ,$$

$$A_{01}=0\ ,$$

$$B_{10}=-10a+2s(5-4s^2)a^2-(\tfrac{5}{2}-6s^2)a^3\ ,$$

$$B_{01}=-4s(5-4s^2)a+(5-4s^2)a^2-2s(1-2s^2)a^3\ ,$$

$$D=20-8s(5-6s^2)a+10(1-2s^2)a^2+s(1-4s^2)a^3\ ,$$

$$s=\sin\alpha\ .$$

A second application of (92) gives the third-order terms

$$x^{*(2)}(u,v)=x^{*(1)}(u,v)+A_{30}u^3+A_{12}uv^2+O(|\mathbf{u}|^5)\ , \tag{97}$$

$$y^{*(2)}(u,v)=y^{*(1)}(u,v)+B_{30}u^3+B_{21}u^2v+B_{12}uv^2+B_{03}v^3+O(|\mathbf{u}|^5)\ . \tag{98}$$

The explicit analytic expressions for the coefficients are complicated and not particularly instructive. We list some representative numerical values for five values of a in Table I. We note that the coefficients of u,v vanish for $a\to 0$, whereas the cubic terms do not. In this limit, process (92) is nothing but an iterative method for solving the transcendental equations

$$\frac{\partial H_5(\eta(u,v)+\xi(x,y))}{\partial x}=\frac{\partial H_5(\eta(u,v)+\xi(x,y))}{\partial y}=0\ ,$$

with

$$H_5(\zeta)\equiv\sum_{k=0}^{4}\cos\zeta_k\ .$$

VII. DIFFRACTION PATTERN

The diffraction pattern of the set of quasicenters of tolerance ϵ is the Fourier transform of the density function $\rho_\epsilon(\mathbf{x})$ consisting of a sum of δ functions of unit weight:

$$\rho_\epsilon(\mathbf{x})=\sum_\nu\delta^2(\mathbf{x}-\mathbf{x}_\nu^*)\ , \tag{99}$$

where the sum is over all integer lattice points $\nu\in Z^5$ such that $|\phi_U(2\pi\nu)|\le\epsilon$, $\phi_W(2\pi\nu)=0$, and $\mathbf{x}_\nu^*$ is the unique quasicenter of tolerance ϵ associated with $2\pi\nu$. The density is the restriction to X of the generalized function

$$f(\zeta)=\sum_{\nu\in Z^5}f_0(\zeta+2\pi\nu)\ , \tag{100}$$

TABLE I. Coefficients appearing in Eqs. (97) and (98), for five values of the parameter a.

Coefficient \ a	0	0.1	0.3	0.5	0.7
A_{10}	0	−0.040 797 3	−0.113 159	−0.175 368	−0.229 422
A_{30}	1/24	0.041 272 8	0.038 927 9	0.035 657 7	0.032 186 9
A_{12}	−1/8	−0.105 816	−0.077 320 3	−0.057 802 9	−0.044 073 3
B_{10}	0	−0.047 960 1	−0.133 026	−0.206 158	−0.269 702
B_{01}	0	−0.025 214 1	−0.069 936	−0.108 384	−0.141 791
B_{30}	0	0.005 290 8	0.011 598	0.014 450 7	0.015 425 7
B_{21}	1/8	0.113 098	0.093 283 6	0.077 692 7	0.065 304 9
B_{12}	0	0.005 290 8	0.011 598	0.014 450 7	0.015 425 7
B_{03}	−1/24	−0.033 990 7	−0.022 964 6	−0.015 768	−0.010 955 3

$$f_0(\zeta(x,y,u,v,w))=\delta^2(\mathbf{x}-\mathbf{x}^*(u,v)) \times\theta(\epsilon^2-\tfrac{5}{2}(u^2+v^2)) \times\theta(\epsilon^2-w^2)\ . \tag{101}$$

Note that the support of f_0 is not contained in the full three-dimensional fixed-point manifold, but does have the correct intersection for $w=0$. The advantage is a simple w dependence for f_0. As a consequence of the periodicity of $f(\zeta)$, we can expand it as a Fourier series,

$$f(\zeta)=\sum_{\mu\in Z^5} c_\mu e^{i\mu\cdot\zeta}\ , \tag{102}$$

where, assuming ϵ sufficiently small that $\mathrm{supp} f_0\subset[-\pi,\pi]^5$,

$$c_\mu=(2\pi)^{-5}\int d^5\zeta e^{-i\mu\cdot\zeta}f_0(\zeta) \tag{103}$$

$$=\gamma\int dx\,dy\,du\,dv\,dw\,\theta(\epsilon^2-\tfrac{5}{2}(u^2+v^2))\theta(\epsilon^2-w^2) \times\delta^2(\mathbf{x}-\mathbf{x}^*(u,v))\exp[-i(k_x(\mu)x+\cdots +k_w(\mu)w)]\ , \tag{104}$$

with

$$k_x(\mu)=\mu\cdot\omega^{(1)},\quad k_y(\mu)=\mu\cdot\omega^{(2)},\quad k_u(\mu)=\mu\cdot\omega^{(3)}\ ,$$
$$k_v(\mu)=\mu\cdot\omega^{(4)},\quad k_w(\mu)=\mu\cdot\omega^{(5)}=\sum_{i=0}^{4}\mu_i\ ,$$
$$\gamma=5^{5/2}2^{-7}\pi^{-5}\ .$$

On the other hand,

$$\rho_\epsilon(\mathbf{x})=f(\xi(\mathbf{x}))=\sum_\mu c_\mu e^{i\mu\cdot\xi(\mathbf{x})}=\sum_\mu c_\mu e^{i\mathbf{k}_\parallel(\mu)\cdot\mathbf{x}}\ , \tag{105}$$

where

$$\mathbf{k}_\parallel(\mu)=(k_x(\mu),k_y(\mu))\ .$$

Since $\mathbf{k}_\parallel(\mu)$ determines μ only up to an arbitrary multiple of $\omega^{(5)}=(1,1,1,1,1)$ [10], each distinct exponential in (105) corresponds to an equivalence class of $\mu \bmod\omega^{(5)}$, which we denote $\bar\mu$, with coefficient

$$c_{\bar\mu}=\sum_{p=-\infty}^{\infty} c_{\mu+p\omega^{(5)}},\quad \mu\in\bar\mu\ . \tag{106}$$

Since in (104) $k_u(\mu)$, $k_v(\mu)$, and $\mathbf{k}_\parallel(\mu)$ depend only on the equivalence class of μ, the sum in (106) can be carried out explicitly:

$$c_{\bar\mu}=\hat\gamma\int du\,dv\,\theta(\hat\epsilon^2-u^2-v^2) \times\exp[-i(k_u(\mu)+k_v(\mu) +\mathbf{k}_\parallel(\mu)\cdot\mathbf{x}^*(u,v))]\ , \tag{107}$$

where

$$\hat\gamma=5^{3/2}2^{-6}\pi^{-4}\ ,$$
$$\hat\epsilon=\sqrt{\tfrac{2}{5}}\epsilon\ .$$

To evaluate $c_{\bar\mu}$, we need to insert the fixed-point functions $x^*(u,v)$ and $y^*(u,v)$ in (107). First let us do this in the first-order approximation [(95),(96)]. Introducing

$$\hat k_u=k_u+A_{10}k_x,\quad \hat k_v=k_v+B_{10}k_x+B_{01}k_y\ ,$$

we have

$$c_{\bar\mu}=\hat\gamma\int du\,dv\,\theta(\hat\epsilon^2-u^2-v^2)\exp[-i(\hat k_u(\mu)+\hat k_v(\mu))]$$
$$=2\hat\gamma\hat\epsilon^2\frac{J_1(\hat k\hat\epsilon)}{\hat k\hat\epsilon} \tag{108}$$

with

$$\hat k=\sqrt{\hat k_u^2+\hat k_v^2}\ .$$

Let us go to one additional order in the expansion of $\mathbf{x}^*(u,v)$. Substituting into (107) and truncating at the cubic terms give

$$c_{\bar\mu}=\hat\gamma\int d\mathbf{u}\,\theta(\hat\epsilon^2-\mathbf{u}^2)\left[1+k_x\sum_{m+n=3}A_{mn}\left[i\frac{\partial}{\partial\hat k_u}\right]^m\left[i\frac{\partial}{\partial\hat k_v}\right]^n +k_y\sum_{m+n=3}B_{mn}\left[i\frac{\partial}{\partial\hat k_u}\right]^m\left[i\frac{\partial}{\partial\hat k_v}\right]^n\right]e^{-i\hat{\mathbf{k}}\cdot\mathbf{u}} \tag{109}$$

$$=2\hat\gamma\hat\epsilon^2\left[\frac{J_1(\hat k\hat\epsilon)}{\hat k\hat\epsilon}+g(\hat k\hat\epsilon)\hat\epsilon^4(3\hat k_uC_{30}+3\hat k_vC_{03}+\hat k_vC_{21}+\hat k_uC_{12}) +h(\hat k\hat\epsilon)\hat\epsilon^6(\hat k_u^3C_{30}+\hat k_v^3C_{03}+\hat k_u^2\hat k_vC_{21}+\hat k_u\hat k_v^2C_{12})\right]\ , \tag{110}$$

where

$$g(z)=-\frac{4}{x^2}J_0(z)+\left[-\frac{1}{z^3}+\frac{8}{z^5}\right]J_1(z),\quad h(z)=\left[-\frac{1}{z^4}+\frac{24}{z^6}\right]J_0(z)-\frac{48}{z^7}J_1(z)\ ,$$
$$C_{mn}(\bar\mu)=-i(k_x(\bar\mu)A_{mn}+k_y(\bar\mu)B_{mn})\ .$$

In the Hamiltonian limit $a\to0$, (110) reduces to

$$c_{\bar{\mu}}=2\hat{\gamma}\hat{\epsilon}^2\left|\frac{J_1(\hat{k}\hat{\epsilon})}{\hat{k}\hat{\epsilon}}+\frac{i}{24}h(\hat{k}\hat{\epsilon})\hat{\epsilon}^6(-k_xk_u^3+k_yk_v^3-3k_yk_u^2k_v+3k_xk_v^2k_u)\right| . \tag{111}$$

As a simple application of the density function $\rho_\epsilon(\mathbf{x})$ and its Fourier transform, we can easily determine the average spacing d_ϵ of the quasicenters in the plane. This is just $1/\sqrt{N_\epsilon}$, where N_ϵ is the average number of quasicenters per unit area of phase space, given by

$$N_\epsilon=\lim_{A\to\infty}\frac{\int_A\rho_\epsilon(\mathbf{x})d\mathbf{x}}{\int_A d\mathbf{x}}=c_{(0,0,0,0,0)}=\frac{\sqrt{5}\epsilon^2}{32\pi^3} . \tag{112}$$

Thus

$$d_\epsilon=2^{5/2}\pi^{3/2}5^{-1/4}\epsilon^{-1} . \tag{113}$$

Note that these are exact statistical results for averages over all phase space, not simply approximate results for small ϵ. For $\epsilon=0.2$, formula (112) predicts that there should be about $1500^2\times N_{0.2}=202.828$ quasicenters displayed in Fig. 5. The actual count is 207.

Similar reasoning allows us to calculate $N_H(\delta E)$, the number of quasicenters per unit area that have energies [i.e., values of $H(x,y)$ in (3)] within δE of the maximum value, 5. The density of such quasicenters is the restriction to subspace X of a generalized function f_H defined by

$$f_H(\zeta)=\sum_{\nu\in Z^5}f_{H0}(\zeta+2\pi\nu) , \tag{114}$$

$$f_H(\zeta(x,y,u,v,w)) \tag{115}$$
$$=\delta^2(\mathbf{x}-\mathbf{x}^*(u,v))$$
$$\times\theta\left[\delta E-5+\sum_{i=0}^{4}\cos\zeta_i(x,y,u,v,w)\right]\theta(\epsilon'^2-w^2) . \tag{116}$$

Then

$$N_H(\delta E)=\hat{\gamma}\int du\,dv\,\theta(\delta E-\tilde{H}(u,v)) , \tag{117}$$

where

$$\tilde{H}(u,v)=5-\sum_{i=0}^{4}\cos[\zeta_i(x^*(u,v),y^*(u,v),u,v,0)] . \tag{118}$$

The integral in (117) just calculates the area enclosed by the contour $\tilde{H}(u,v)=\delta E$. For small δE, the latter asymptotically becomes an ellipse, so that

$$N_H(\delta E)=\frac{\pi\hat{\gamma}\delta E}{\sqrt{\det\mathbf{F}}}+O((\delta E)^3) , \tag{119}$$

where the matrix F, defined by

$$\tilde{H}(u,v)=\mathbf{u}\cdot\mathbf{F}\cdot\mathbf{u}+O(|\mathbf{u}|^4) . \tag{120}$$

Explicitly,

$$F_{ij}=\tfrac{1}{2}\sum_{k=0}^{4}f_{ki}f_{kj} , \tag{121}$$

where

$$f_{ku}=\cos\frac{4\pi k}{5}+A_u\cos\frac{2\pi k}{5}+B_u\sin\frac{2\pi k}{5} ,$$

$$f_{kv}=\sin\frac{4\pi k}{5}+B_v\sin\frac{2\pi k}{5} ,$$

with A_{10}, B_{10}, B_{01} given in (96). For the asymptotically small parameter a the result is particularly simple:

$$\lim_{a\to 0}N_H(\delta E)=(2\pi)^{-4}\pi\sqrt{5}\delta E+O((\delta E)^2) . \tag{122}$$

This gives an analytic expression for the high end of the elliptical fixed-point distribution found empirically in [3].

VIII. COMPUTER-ASSISTED CONVERGENCE PROOF

For fixed a and ϵ, the existence of a quasiperiodic lattice of quasicenters of tolerance ϵ can be proven rigorously by establishing the convergence of the iterative scheme [see (91)–(94)]

$$\mathbf{x}^{(0)}=\mathbf{0} , \tag{123}$$

$$\mathbf{x}^{(n+1)}=\mathbf{x}^{(n)}+\delta\mathbf{x}^{(n)} , \tag{124}$$

$$\delta\mathbf{x}^{(n)}\equiv G_0[\tilde{M}_\zeta^{(5)}(\mathbf{x}^{(n)}-\mathbf{x}^{(n)})] , \tag{125}$$

for all $\zeta\in U$ with $|\zeta|\le\epsilon$. By virtue of the quasiperiodicity, establishing the convergence criterion in the neighborhood of the origin suffices to establish its validity everywhere in the plane.

Our strategy is to obtain bounds on $|\delta\mathbf{x}^{(n)}|$ that tend to zero for $n\to\infty$ with sufficient rapidity that the existence of $\lim\mathbf{x}^{(n)}$ can be inferred. For this purpose we need a recursion relation for $\delta\mathbf{x}^{(n)}$, which can be derived from (124) and (125) as follows. First we apply $\tilde{M}_\zeta^{(5)}$ on $\mathbf{x}^{(n+1)}$ and expand in a Taylor series:

$$\tilde{M}_\zeta^{(5)}(\mathbf{x}^{(n+1)})=\tilde{M}_\zeta^{(5)}(\mathbf{x}^{(n)}+\delta\mathbf{x}^{(n)})$$
$$=\tilde{M}_\zeta^{(5)}(\mathbf{x}^{(n)})+D\tilde{M}_\zeta^{(5)}(\mathbf{x}^{(n)})\cdot\delta\mathbf{x}^{(n)}$$
$$+\tfrac{1}{2}\delta\mathbf{x}^{(n)}\cdot D^2\tilde{M}_\zeta^{(5)}(\mathbf{x}^{(n)}+\Delta\mathbf{x}^{(n)})\cdot\delta\mathbf{x}^{(n)} , \tag{126}$$

where $\Delta\mathbf{x}^{(n)}$ lies in the closed rectangle spanned by $\mathbf{0}$ and $\delta\mathbf{x}^{(n)}$ (i.e., with $\mathbf{0}$ and $\delta\mathbf{x}^{(n)}$ at opposite corners) and $D^2\tilde{M}_\zeta^{(5)}(\mathbf{x})$ is the matrix of second derivatives of $\tilde{M}_\zeta^{(5)}$ evaluated at $\mathbf{x}$. A dot represents the contraction of a derivative index with that of $\delta\mathbf{x}^{(n)}$. Rearranging terms in (126) and multiplying from the left by G_0 leads to

$$\delta\mathbf{x}^{(n+1)}=G_0[(D\tilde{M}_\zeta^{(5)}(\mathbf{x}^{(n)})-DM^5(\mathbf{0}))\cdot\delta\mathbf{x}^{(n)}$$
$$+\tfrac{1}{2}\delta\mathbf{x}^{(n)}\cdot D^2\tilde{M}_\zeta^{(5)}(\mathbf{x}^{(n)}+\Delta\mathbf{x}^{(n)})\cdot\delta\mathbf{x}^{(n)}] . \tag{127}$$

The convergence problem can be stated rather simply

with the aid of interval analysis [21]. The method allows one to obtain rigorous bounds on any function of real variables x,y constructed using elementary rules of addition, subtraction, multiplication, and division. The idea is to extend these arithmetic operations to closed intervals in such a way that worst-case bounds are always respected. For our purpose we must add to the list of rules (see Appendix) ones giving bounds to the sine and cosine of an interval.

The concept of bounding interval generalizes easily to higher dimensions. An ordered pair (two-vector) $([x_1,x_2],[y_1,y_2])$ thus represents a bounding rectangle with corners at (x_1,y_1), (x_1,y_2), (x_2,y_1), and (x_2,y_2) in the xy plane. Similarly, an ordered n-tuplet of closed intervals represents a bounding n-dimensional parallelepiped. In other words, an ordered n-tuplet of intervals is just another way of writing a direct product of the intervals. To facilitate the operations of interval analysis, we prefer the ordered-multiplet notation in this section.

Let us start with $\mathbf{x}^{(n)}\in\mathcal{S}$, $\delta\mathbf{x}^{(n)}\in\mathcal{T}$, where $\mathcal{S}$ and $\mathcal{T}$ are bounding rectangles. We can then calculate a bounding rectangle $\mathcal{S}^{(n+1)}$ for $\mathbf{x}^{(n+1)}$ defined by (124) as

$$\mathcal{S}^{(n+1)}=\mathcal{S}+\mathcal{T}\ , \tag{128}$$

in the sense of interval addition (see Appendix). Moreover, we obtain a bounding rectangle $\mathcal{T}^{(n+1)}$ for $\delta\mathbf{x}^{(n+1)}$ based on (127),

$$\mathcal{T}^{(n+1)}=G[(DM^5(\mathcal{S})-DM^5(\mathbf{0}))\cdot\mathcal{T} +\tfrac{1}{2}\mathcal{T}\cdot D^2M^5(\mathcal{S}^{(n+1)})\cdot\mathcal{T}]\ . \tag{129}$$

Again, the right-hand side has meaning in the sense of interval arithmetic, once we have given a specific representation of DM^5 and D^2M^5 in terms of elementary algebraic and trigonometric operations. Any of the many equivalent representations will do, but of course some will give better bounds than others. In order to prove the convergence of our fixed point search, it is sufficient to show that iteration of the mapping of bounding rectangles defined by (128) and (129) converges to a limit, with

$$\lim_{n\to\infty}\mathcal{T}_n=\mathcal{O}\equiv[0,0]\times[0,0]\ .$$

The idea is illustrated in Fig. 8.

To apply the technique just described for arbitrary $\zeta\in U$ with $|\zeta|\le\epsilon$, it is convenient to go over to a five-dimensional (5D) formalism. We therefore set up a recursive scheme for bounding 5D parallelepipeds $\mathcal{Z}^{(n)}$ [for $\zeta+\xi(\mathbf{x}^{(n)})$] and bounding rectangles $\mathcal{T}^{(n)}$ (for $\delta\mathbf{x}^{(n)}$). Noting the identities

$$DM^5(\mathbf{x})=D\tilde{M}^5_z(\mathbf{0})+I,\quad D^2M^5(\mathbf{x})=D^2\tilde{M}^5_z(\mathbf{0})\ , \tag{130}$$

where

$$z=(z_0,\ldots,z_4),\quad z_k=2\pi\langle\langle\,\mathbf{e}_k\cdot\mathbf{x}/2\pi\,\rangle\rangle\ ,$$

and I is the two-dimensional identity matrix, we get, in place of (128) and (129),

$$\mathcal{Z}^{(n+1)}_k=\mathcal{Z}^{(n)}_k+\mathbf{e}_k\cdot\mathcal{V}^{(n)},\quad k=0,\ldots,4\ , \tag{131}$$

$$\mathcal{T}^{(n+1)}=G[(D\tilde{M}^5_{\mathcal{Z}^{(n)}}(\mathbf{0})-D\tilde{M}^5_{\mathcal{O}}(\mathbf{0}))\cdot\mathcal{V}^{(n)} +\tfrac{1}{2}\mathcal{T}^{(n)}\cdot D^2\tilde{M}^5_{\mathcal{Z}^{(n+1)}}(\mathbf{0})\cdot\mathcal{T}^{(n)}]\ . \tag{132}$$

Our strategy is to iterate (131) and (132) N times to reduce the size of the bounding rectangle $\mathcal{T}$ to $\mathcal{T}_N$ and to arrive at an intelligent guess for a single $\mathcal{Z}^{(\infty)}$ to serve as a fixed 5D parallelepiped for all remaining iterations. For $n>N$, we replace (132) by

$$\mathcal{T}^{(n+1)}=\mathcal{L}\mathcal{T}^{(n)}\ , \tag{133}$$

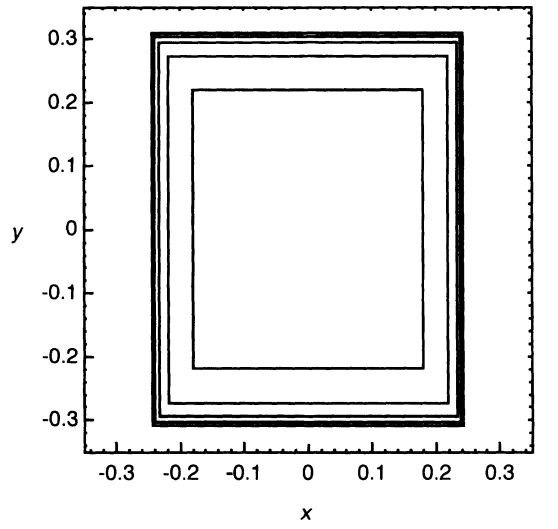

(a)

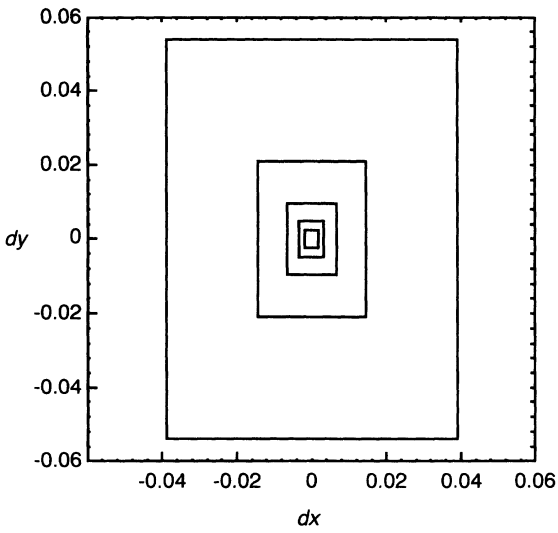

(b)

FIG. 8. Sequence of bounding rectangles (a) $\mathcal{S}$, for position $\mathbf{x}$, and (b) $\mathcal{T}$, for displacement $\delta\mathbf{x}$. The case pictured here is taken from our actual calculations for $a=0.3$, $\epsilon=0.075$. We see the apparent convergence of $\mathcal{S}$ to a limiting rectangle, and the convergence to the origin of $\mathcal{T}$. Interval analysis confirms that the iterative scheme is indeed convergent in this case (see Table II).

TABLE II. Rigorous lower bounds on $\epsilon_{\rm crit}$ for selected parameter values. For all quasicenters of tolerance less than $\epsilon_{\rm crit}$, the iterative scheme is guaranteed to converge.

a	0.1	0.2	0.3	0.4	0.5	0.6	0.7
$\epsilon_{\rm crit}$	0.17	0.11	0.075	0.052	0.035	0.024	0.017

where $\mathcal{L}$ is the interval matrix

$$\mathcal{L}=G[(D\tilde{M}^5_{\mathcal{Z}^{(\infty)}}(\mathbf{0})-D\tilde{M}^5_O(\mathbf{0}))+\tfrac{1}{2}\mathcal{T}^{(N)}\cdot D^2\tilde{M}^5_{\mathcal{Z}^{(\infty)}}(\mathbf{0})] \ . \tag{134}$$

We are through if we can show that the eigenvalues of $\mathcal{L}$ are less than unity in magnitude and that the $\mathcal{Z}^{(n)}$, $n>N$, all remain within $\mathcal{W}^{(\infty)}$. A bound λ for the eigenvalues may be calculated as

$$\lambda=\lim_{\mathcal{T}\in S}\|\mathcal{L}\mathcal{V}\| \ , \tag{135}$$

where S is the set of edges of the square $([-1,1],[-1,1])$,

$$S=\{([1,1],[-1,1]),([-1,1],[1,1]),([-1,-1,],[-1,1]),([-1,1,],[-1,-1])\} \ ,$$

and, for an arbitrary bounding rectangle $\mathcal{T}=([a,b],[c,d])$, we define

$$\|\mathcal{T}\|=\sup_{\mathbf{x}\in\mathcal{T}}|\mathbf{x}|=\max\{\sqrt{a^2+c^2},\sqrt{a^2+d^2},\sqrt{b^2+c^2},\sqrt{b^2+d^2}\} \ .$$

With the aid of MATHEMATICA (version 2.1 for the Macintosh) we have programmed the rules of interval arithmetic listed in the Appendix and tested the convergence of the iterative scheme (131) and (132) for selected values of the parameter a and the tolerance ϵ. In each case we started off the process with a bounding 5D hypercube $\mathcal{Z}^{(0)}$ of side $[-\epsilon,\epsilon]$ and calculated

$$\mathcal{T}^0=G\tilde{M}^5_{\mathcal{Z}^{(0)}}(\mathbf{0}) \ .$$

After iterating (131) and (132) five times, if the process appeared to be converging, we estimated a common bounding 5D region $\mathcal{Z}^{(\infty)}$ for the remaining iterations, calculated a bound λ on the contraction rate as in (135), and checked that all remaining $\mathcal{Z}^{(n)}$ were indeed bounded by the conjectured $\mathcal{Z}^{(\infty)}$. In Table II we list, for selected values of a, the largest values of ϵ for which we were able to establish convergence. In each case, we estimate that the actual critical ϵ is no more than 10% larger than the rigorous lower bound listed in the table.

As is almost always the case, rigorous bounds established by interval arithmetic are very conservative. To explore the actual situation for the process (124) and (125), we made a numerical convergence check for all projected lattice points of tolerance 0.3 within the parallelogram

$$0\le\mathbf{e}_k\cdot\mathbf{x}<600\pi, \quad k=0,2 \ ,$$

for parameter values $a=0.1,0.2,\ldots,0.7$. As one can estimate from formula (112), there are over 1200 such points, and if one includes all images under the map M and the inversion operator, the results actually apply to ten times as many points. The iterative scheme was found to converge, with an accuracy of 10^{-12}, in every case.

IX. REMARKS

A fascinating aspect of the stochastic web is the *dynamical generation of quasicrystalline structure.* Here one usually refers [12] to the geometry of the web itself, a network of narrow channels traced out by a single unbounded chaotic orbit. In the present work we have treated a far simpler manifestation of the long-range quasicrystalline order, namely, the quasiperiodic lattice of fixed points called quasicenters. These are replicas of the origin of coordinates with respect to the action of the map. By choosing a suitable translation vector, one can always find a quasicenter that mimics the true origin with arbitrarily high accuracy over the entire phase plane. The situation is similar to, but not equivalent to, the local isomorphism property [7] of the Penrose tiling (the latter is an exact congruence of finite parts of the tiling). Although the lattice of quasicenters is only part of the whole story, it provides an important milestone on the road to a comprehensive understanding of the web map's quasicrystalline structure.

ACKNOWLEDGMENT

I would like to thank G. M. Zaslavsky for helpful discussions.

APPENDIX

The basic ideas of interval arithmetic are set forth in Ref. [21]. An *interval* is simply a closed interval on the real line, labeled by its end points, e.g., $[a,b]$. The following rules give worst-case bounds for the elementary operations of arithmetic as applied to elements of the respective intervals [21]:

$$[a,b]+[c,d]=[c,d]+[a,b]=[a+c,b+d]\ ,$$

$$[a,b]\times[c,d]=[c,d]\times[a,b]$$
$$=[\min\{ac,ad,bc,bd\},\max\{ac,ad,bc,bd\}]\ ,$$

$$a+[b,c]=[b,c]+a=[a,a]+[b,c]\ ,$$

$$a\cdot[b,c]=[b,c]\cdot a=[a,a]\cdot[b,c]\ ,$$

$$[a,b]-[c,d]=[a,b]+(-1)\cdot[c,d]\ ,$$

$$[a,b]/[c,d]=[a,b]\cdot[c,d]^{-1}\ .$$

These are supplemented by rules for integer powers (in the following, n is a positive integer):

$$[a,b]^n=\begin{cases}[0,\max\{a^n,b^n\}], & n \text{ even},\ 0\in[a,b]\\ [\min\{a^n,b^n\},\max\{a^n,b^n\}] & \text{otherwise}\ ,\end{cases}$$

$$[a,b]^0=[1,1]\ ,$$

$$[a,b]^{-1}=\begin{cases}[-\infty,\infty], & 0\in[a,b]\\ [\min\{1/a,1/b\},\max\{1/a,1/b\}] & \text{otherwise},\end{cases}$$

$$[a,b]^{-n}=([a,b]^n)^{-1}\ .$$

Finally, we need useful bounds for the sine and cosine functions when their arguments are reasonably close to an integer multiple of 2π. For this purpose we replace the irrational π by the interval $[\pi^+,\pi^-]$ $\equiv[31\,415\,926\,535\,897\,932\times10^{-16},31\,415\,926\,535\,897\,933\times10^{-16}]$:

$$\sin([0,0])=[0,0],\quad \cos([0,0])=[1,1]\ .$$

For $-\pi^+<a<\pi^+$,

$$\sin([a,b])=\begin{cases}[s_a,s_b], & a,b\in[-1,1]\\ [-1,1] & \text{otherwise}\ ,\end{cases}$$

$$\cos([a,b])=\begin{cases}[c_a,c_b], & a,b\in[-1,1]\\ [-1,1] & \text{otherwise}\ ,\end{cases}$$

where

$$s_a=a-\frac{a^3}{6}+\begin{cases}a^5/120, & a<0\\ 0, & a\geq0\ ,\end{cases}$$

$$s_b=b-\frac{b^3}{6}+\begin{cases}0, & b<0\\ b^5/120, & b\geq0\ ,\end{cases}$$

$$c_a=\min\{1-a^2/2+a^4/24-a^6/720,1-b^2/2+b^4/24-b^6/720\}\ ,$$

$$c_b=\begin{cases}1, & a\leq0 \text{ and } b\geq0\\ \max\{1-a^2/2+a^4/24,1-b^2/2+b^4/24\} & \text{otherwise}\ .\end{cases}$$

For $a\leq-\pi^+$, we use

$$\sin([a,b])=\sin([a+\pi^-,b+\pi^+])$$

and for $a\geq\pi^+$, we use

$$\sin([a,b])=\sin([a-\pi^+,b-\pi^-])\ ,$$

and analogous formulas for the cosine.

We restrict ourselves to exact operations on rational numbers. For the sake of efficiency, we follow each operation with worst-case rounding of the interval end points to rational numbers of the form $q\times10^n$, where q is an integer with at most five digits.

We implement our rules of interval arithmetic using MATHEMATICA (trademark, Wolfram Research, Inc.), version 2.1, on a Macintosh IIci personal computer. A similar approach, with rounding of floating-point numbers, is used in the MATHEMATICA package "Interval Analysis."

[1] G. M. Zaslavskii, M. Yu. Zakharov, R. Z. Sagdeev, D. A. Usikov, and A. A. Chernikov, Zh. Eksp. Teor. Fiz. **91**, 500 (1986) [Sov. Phys. JETP **64**, 294 (1986)].

[2] G. M. Zaslavskii, M. Yu. Zakharov, R. Z. Sagdeev, D. A. Usikov, and A. A. Chernikov, Pis'ma Zh. Eksp. Teor. Fiz. **44**, 349 (1986) [JETP Lett. **44**, 451 (1986)].

[3] G. M. Zaslavskii, R. Z. Sagdeev, D. A. Usikov, and A. A. Chernikov, Usp. Fiz. Nauk. **156**, 193 (1988) [Sov. Phys. Usp. **31**, 887 (1988)].

[4] R. Penrose, Bull. Inst. Math. Appl. **10**, 266 (1974).

[5] R. Ammann (unpublished), cited in B. Grünbaum and G. C. Shephard, *Tilings and Patterns* (Freeman, New York, 1987).

[6] N. G. de Bruijn, Proc. Nederl. Akad. Wetensch. **A84**, 27 (1981); **A84**, 38 (1981); **A84**, 53 (1981).

[7] D. Levine and P. J. Steinhardt, Phys. Rev. B **34**, 596 (1986).

[8] N. G. de Bruijn, Proc. Nederl. Akad. Wetensch. **A89**, 123 (1986).

[9] J. H. Lowenstein, Phys. Rev. E **47**, R3811 (1993).

[10] J. H. Lowenstein, Chaos **2**, 413 (1992).

[11] G. M. Zaslavsky, Chaos **1**, 1 (1991).

[12] G. M. Zaslavskii, R. Z. Sagdeev, D. A. Usikov, and A. A. Chernikov, *Weak Chaos and Quasiregular Patterns* (Cambridge University, Cambridge, England, 1991).

[13] W. Rudin, *Fourier Analysis on Groups* (Interscience, New

York, 1962), p. 32.
[14] L. Schwartz, *Théorie des Distributions* (Hermann, Paris, 1957).
[15] I. M. Gel'fand and G. E. Shilov, *Generalized Functions*, translated by E. Saletan (Academic, New York, 1967), Vol. 1.
[16] V. Elser, Acta Crystallogr. A **42**, 36 (1986).
[17] R. K. P. Zia and W. J. Dallas, J. Phys. A **18**, L341 (1985).
[18] M. Duneau and A. Katz, Phys. Rev. Lett. **54**, 2688 (1985).
[19] P. A. Kalugin, A. Kitaev, and L. Levitov, Pis'ma Zh. Eksp. Teor. Fiz. **41**, 119 (1985) [JETP Lett. **41**, 145 (1985)].
[20] J. E. S. Socolar and P. J. Steinhardt, Phys. Rev. B **34**, 617 (1986).
[21] R. E. Moore, *Interval Analysis* (Prentice-Hall, Englewood Cliffs, NJ, 1966).